Environmental Science and Pollution Research
https://doi.org/10.1007/s11356-018-1504-6

RESEARCH ARTICLE

Sulfur removal from model fuel by Zn impregnated retorted shale and with assistance of design of experiments

Flávia Melo de Lima[1] · Talitha de Andrade Borges[2] · Renata Martins Braga[3] · Dulce Maria de Araújo Melo[4] · Antônio Eduardo Martinelli[1]

Received: 2 November 2017 / Accepted: 6 February 2018

Abstract
There is global concern about acid rain and other pollution which is caused by the consumption of oil. By decreasing sulfur content in the oil, we can reduce unwanted emissions and acid rain. Shale was used which is a solid waste generated in the pyrolysis of shale, impregnated with Zn as an adsorbent which removes sulfur present in fuels from the hexane/toluene model solution. An influence of the agitation time (60–180 min), temperature (25–35 °C), adsorbent mass (0.1–0.25 g), and initial sulfur concentration (100–250 ppm) factorial 24 with three central points totaling 19 experiments was applied to investigate the effect of the variables on the efficiency of sulfur removal in fuels. The values of the parameters tested for maximum sulfur removal were obtained as follows: contact time = 180 min, temperature = 35 °C, adsorbent mass = 0.25 g, and initial sulfur concentration = 100 ppm. The mathematical model proposed with R^2 99.97% satisfied the experimental data. This may provide a theoretical basis for new research and alternative uses for tailings of schist industrialization in order to evaluate its potential.

Keywords Adsorption · Retorted shale · Fuel · Sulfur · Factorial design · Statistic

Introduction

Environmental pollution caused by inorganic and organic contaminants has steadily increased in parallel with world population, industrialization, and urbanization, especially in developing countries (Ahmad et al. 2011). There are several categories of air pollutants that are currently regulated by federal and state governments or are of concern to the environment or public health. These include sulfur oxides (SOx), nitrogen oxides (NOx), lead (Pb), carbon monoxide (CO), ozone, and particulate matter (PM) (Iberahim et al. 2017).

Due to these concerns, environmental regulations focus attention on the reduction of emissions from the transport sector with the aim of improving air quality. There has been an increase in the environmental requirements related to emissions of sulfur oxides (SOx), which are formed by the combustion of sulfur components present in fuels (Song 2003; Li et al. 2013; Nejad and Beigi 2015). Removal of sulfur from fuels has gained importance since global governments are determined to reduce sulfur in diesel and gasoline by 15 and 30 ppm from the levels at the end of the twentieth century at around 430 and 130 ppm respectively (Oyama et al. 2009).

In the USA, the legal limit of sulfur content of most fuels was reduced from 500 to 15 ppm in 2006. In Europe, the limits of gasoline and diesel fuels were reduced to 10 ppm in 2010. Following this trend, Japan reduced the limit from 500 to 50 ppm in 2004 and then to 10 ppm in 2007 (USEPA 2000; Stanislaus et al. 2010; Baeza et al. 2012). In 2009, the legal limit in Brazil was made to be 30 to 50 ppm (ANP 2016). Therefore, the desulfurization of transport fuels has become an important issue throughout the world.

Responsible editor: Guilherme L. Dotto

✉ Flávia Melo de Lima
flaviamdl@hotmail.com

[1] Universidade Federal do Rio Grande do Norte, PPGCEP – CCET, Natal, Rio Grande do Norte 59078-970, Brazil

[2] Universidade Federal do Rio Grande do Norte, Natal 59078-970, Rio Grande do Norte, Brazil

[3] Universidade Federal do Rio Grande do Norte, Escola Agrícola de Jundiaí - EAJ, Macaíba, Rio Grande do Norte 59280-000, Brazil

[4] Universidade Federal do Rio Grande do Norte, Instituto de Química, Natal, Rio Grande do Norte 59078-970, Brazil

Published online: 05 March 2018

Many of the control and treatment technologies have been developed to monitor and eliminate the emission of toxic gases and to eliminate their risks to humans and the environment (Ibrahim et al. 2016). The restrictive scenario is justified by the fact that such gases (SOx) cause environmental impacts, such as acid rain, characterized by the precipitation of sulfuric acid together with rain (Zhang et al. 2017; Bhatia and Sharma 2012). This causes several problems for humans which range from diseases such as bronchitis, asthma, rhinitis, and cardiovascular diseases among others. It also causes genetic mutations and alterations in plants. In addition to causing genetic mutations and changes in plants and deforestation of forests, it causes acidification of soil and water causing mortality and imbalance of plant and animal species (Topsøe 2003; Ma et al. 2007).

Other industrial factors also justify the need for the processes of desulfurization of fuels. Among these are the reduction or even elimination of corrosion during the refining process, the production of inputs with an acceptable level of odor, the increase of performance and fuel stability, and poisoning of catalysts used both in exhaust gas treatment vehicles and in oil refining processes in the production of the fuel itself, as well as the lower emission of SOx gases (James 2000; He et al. 2016).

Sulfur is present in fuels in the form of elemental sulfur, mercaptans, sulfides, thiophene, benzothiophene, dibenzothiophene, and their alkyl derivatives. Thus, many projects were carried out to concentrate on the desulfurization of thiophene (Zhang et al. 2012; Yu et al. 2015a; Shimoyama and Baba 2016).

Some of the desulfurization techniques reported include the following: extractive desulfurization (EDS) (Dharaskar et al. 2014), oxidative desulfurization (ODS) (Lü et al. 2014), hydrodesulfurization (HDS) (Brunet et al. 2005; Duarte et al. 2011) and adsorption (ADS) (Wu et al. 2014). Some of these techniques have limitations. For example, the extractores used in ODS and EDS processes are generally flammable and contains volatile organic compounds which are also known for having high toxicity, being expensive, being ineffective, and having serious consequences to the environment (Gao et al. 2010; Gui et al. 2010).

During oxidative desulfurization procedure, the refractory sulfur compounds can be transformed into water-soluble products, i.e., thiophene and its lower polarity compounds can be converted to the corresponding sulfoxides/sulfones with higher polarity by strong oxidants, then the sulfones can easily be absorbed or extracted by polar solvents to attain high desulfurization efficiency. ODS is a complementary or alternative technology to HDS (Wei et al. 2016; Wei et al. 2017).

The hydrodesulfurization process is currently used in the petrochemical industry to reduce the content of undesirable sulfur compounds in hydrocarbon fractions. However, the HDS is inefficient for the removal of certain types of sulfur compounds, such as thiophene and its derivatives (Oliveira et al. 2009; Dharaskar et al. 2014).

Thus, adsorption technology appears as an alternative route of desulfurization of fuel as a more ecological method. In order to meet increasingly stringent environmental requirements, special attention has been given to the use of adsorption for the removal of sulfur compounds, which may complement or, in some cases, replace the already existing hydrotreatment processes (Ma et al. 2005; Xiao et al. 2013; Aslam et al. 2017). ADS occurs when the sulfur molecules join the adsorbent and remain there separated from the fuel (Srivastav and Srivastava 2009).

Many studies have focused on ADS because of its low cost, high desulphurization efficiency, loss of low octane numbers, and good market outlook (Wang et al. 2009b; Komarneni et al. 2010). Adsorption is considered a promising technique because it is a simple process, proceeding to operation under ambient temperature and pressure conditions without the need for expensive reagents and catalysts. However, suitable adsorbents are essential for an efficient adsorption process (Tian et al. 2014; Wang et al. 2017).

In addition to some basic characteristics, including high specific area, large pore volume, and suitable pore diameter, to ensure high sulfur adsorption capacity, it is believed that the interaction between sulfur compounds and the adsorbent is the essential factor for high selectivity of desulphurization (Tian et al. 2015).

The specific adsorbents containing transition metals (Ni, Zn, Ag, Ce, and Cu) are known to capture sulfur compounds by complexing adsorbate molecules with free electrons in π orbitals (Velu et al. 2005; Cavalcanti et al. 2015).

Different types of adsorbents, including zeolite (Bhandari et al. 2006; Wang et al. 2009a; Shi et al. 2013), mesoporous silica (Kwon et al. 2008; Li et al. 2012; Teymouri et al. 2013), activated charcoal (Wang and Yang 2007; Yu et al. 2015b; Chen et al. 2016), and metallic and organic structures (Blanco-Brieva et al. 2011; Peralta et al. 2012; Tian et al. 2015) were used for the removal of sulfur compounds from model solutions or fuels.

The Brazilian Shale Industrialization Business Unit (UNSIX) belongs to Petrobras Company and is located in São Mateus do Sul (PR). This unit is under the largest Brazilian shale reserves, Irati Formation, where 7800 t of shale are extracted daily, leading to the generation of solid waste called XR, which accounts for 80–90% of the raw material in the process of shale oil production (Pimentel et al. 2010). There is work on the use of retorted shale as adsorbent of heavy metal in wastewater. Due to its chemical composition constituted mostly by acid, and basic and amphoteric oxides, it assures on the surface of the grains the presence of active groups that can act in the removal of inorganic and organic components (Pimentel et al. 2008).

In this context, the retorted shale was impregnated with Zn and the possibility of using it as an adsorbent to explore its sulfur removal efficiency in fuel was evaluated; a complete factorial design was also performed 2^4 to examine the main effects and the interactions between contact time, temperature, adsorbent mass, and initial sulfur concentration.

Materials and methods

Impregnation and characterization of the adsorbent

In the experiments performed, the retorted shale (0.047–0.077 mm) of S_{BET} specific surface area (65 m^2 g^{-1}), and pore diameter in mesopore range (20 to 500 Å), (Pimentel et al. 2010) was obtained from the Shale Industrialization Business Unit (UN-SIX), located in São Mateus do Sul (PR). For the impregnation of the metal to the shale, zinc nitrate [Zn $(NO_3)_2$] (Alfa Aesar, 99%) was used. Approximately 15 g of retorted shale was added in Erlenmeyer flask (250 mL) containing 100 mL of aqueous solutions containing 0.1 M Zn $(NO_3)_2$, held under constant stirring at 100 rpm shaker for about 12 h at room temperature. After this time, the sample was filtered using qualitative filter paper and washed with distilled water, then dried at 100 °C for 5 h to evaporate the water and obtain the adsorbent material.

The parameters of the immediate analysis were performed in triplicate: moisture content, ash content, volatile matter, and fixed carbon were determined according to the norms ASTM D-3173 (ASTM 2017), ASTM D-3174 (ASTM 2012), ASTM D-3175 (ASTM 2017) e ASTM D-3172 (ASTM 2013), respectively. The elemental chemical composition of Zn-impregnated shale samples was determined by X-ray fluorescence on Philips PM 2400 equipment. Thermal stability was performed on a Shimadzu, DTGA 60, thermocouple in the range of temperature between 25 and 900 °C, heating rate of 5 °C min^{-1}, and in air atmosphere to obtain the thermogravimetric curve. The morphology was observed through micrographs obtained on a scanning electron microscope Shimadzu SSX-550.

Model fuel preparation

The adsorbate chosen to represent the class of sulfur compounds was thiophene P.A. (Sigma-Aldrich, 99%), present in most gasolines, even after the HDS processes. The solvents used in the adsorption tests were n-hexane P.A. (VETEC, 99%), representative of the alkane hydrocarbons present in the carrier fuel, and toluene P.A. (VETEC, 99%), which represents the aromatic hydrocarbons. The initial model fuel was prepared by adding different volumes of thiophene (T) (1000 mg L^{-1}) (2.5, 5, 7.5, 10, 12.5, 15, 17.5, 20, 22.5; 25, 27.5, 30 mL) in volumetric flasks (100 mL). Then 85% of hexane and 15% of toluene were added to the volumetric flasks resulting in 100 mL of thiophene solution having different concentrations (25, 50, 75, 100, 150, 175, 200, 200, 225, 250, 275, 300, 300 L^{-1}).

Adsorption study

Under similar and initial adsorption test conditions, the retorted shale Zn/X showed a 20% increase in thiophene adsorption efficiency in model fuel as compared to retorted shale without Zn. Therefore, Zn/X was used in the development of the adsorption study. Approximately 0.1 g of adsorbent was added in Erlenmeyer with 10 mL of hexane/toluene (85/15) and 250 ppm of S, kept in contact shaking for 300 min at 25 °C, to observe the effect of the adsorption at room temperature avoiding additional operational costs. After this time, the solvent was separated from the shale by filtration; a 2-mL aliquot was reserved for analysis of the sulfur content. The sulfur concentration of 250 ppm was chosen to be higher than permitted.

The sulfur removal of the model fuel was determined from Eq. (1), and the adsorbed amount of sulfur by the adsorbent Zn/X is given by Eq. (2):

$$\%\text{remotion} = \frac{(C_o - C_f)}{C_o} * 100\% \tag{1}$$

$$q = \frac{(C_o - C_f)}{m} * V \tag{2}$$

in which q is the amount of sulfur adhering to the adsorbent (mg L^{-1}), C_0 is the initial sulfur concentration which has been brought into contact with the adsorbent (mg L^{-1}), C_f is the concentration of sulfur (mg L^{-1}) in the solution after adsorption, m is the mass of adsorbent (g), and V is the volume of model fuel placed in contact with the adsorbent (L). The concentrations of sulfur in the solutions before and after the adsorption were analyzed using near-infrared spectrophotometer (NIR), using the NIR model ARCspectro UV-VIS-NIR in diffuse reflectance mode with Fourier transform.

Kinetic and equilibrium models

For better understanding of adsorption process, pseudo first (Eq. (3)) and second-order (Eq. (4)) along with intraparticle diffusion (Eq. (5)) models were applied to describe the thiophene adsorption kinetics over retorted shale (Subhan et al. 2012).

$$\ln(q_e - q_t) = \ln q_e - k_1 t \tag{3}$$

$$\frac{t}{q_t} = \frac{1}{k_2 (q_e)^2} + \frac{t}{q_e} \tag{4}$$

$$q_t = k_i \sqrt{t} + C \tag{5}$$

in which k_1 is the kinetic constant for the pseudo first-order model (min^{-1}), q_e is the quantity adsorbed at equilibrium (mg g^{-1}), t is the contact time (min), q_t is the quantity adsorbed at time t (mg g^{-1}), k_2 is the kinetic constant for the pseudo second-model (g mg^{-1} min^{-1}), k_i is the intraparticle diffusion coefficient (mg g^{-1} $min^{-1/2}$), and C (mg g^{-1}) is related to the thickness of the fluid film surrounding the solid surface.

To evaluate the equilibrium isotherm, the experimental data were fitted by Langmuir (Eq. (6)) and Freundlich (Eq. (7)) models (Subhan et al. 2014).

$$\frac{C_e}{q_e} = \frac{1}{K_L q_{\max}} + \frac{C_e}{q_{\max}} \tag{6}$$

$$\log q_e = \log K_F + \frac{1}{n}\log C_e \tag{7}$$

In which C_e (ppm) is the concentration of the adsorbent in the solution, q_e (mg g^{-1}) is the amount of sulfur adsorbed per gram of adsorbent; $q_{\max}$ (mg g^{-1}) is the maximum adsorption in monolayer and K_L is the Langmuir constant (L mg^{-1}), K_F is the equilibrium constant of the surface adsorption in (mg g^{-1}), and n refers to the interaction between the sites of exchange in the adsorbent and sulfur. A high value for $n > 1$ indicates favorable adsorption.

Factorial design analysis

In this study, we used the full factorial method to evaluate the main effects of experimental factors: contact time (60–180 min), temperature (25–35 °C), adsorbent mass (0.1–0.25 g), initial sulfur concentration (100–250 ppm), and the effects of interactions between these factors. The full factorial planning mechanism involves corrections in all possible combinations with the lower and upper level of each factor. In particular, we used four independent factors, namely time (A), temperature (B), adsorbent mass, (C) and sulfur concentration (D), while sulfur removal efficiency (% removal) was taken as a response. The large factorial design method included 2^4 and 3 replicates at the central point totaling 19 experiments, in order to explore the effect of the main factors and their interactions. The experiments were performed randomly with different levels of all likely combinations of factors. The high (+1) and low (−1) levels of the factors are selected based on preliminary tests and previous results presented in the relevant studies. These values are listed in Table 1. The results of the experimental design were analyzed using the STATISTICA 7.0 Software to investigate the effects, as well as parameters and statistical plans. The interactions between independent variables were analyzed with analysis of variance (ANOVA) and the main effects of the adsorption were identified based on the P value with 95% confidence level.

Table 1 The value of the high (+1) and low (−1) factors of the full factorial planning 2^4

Factor	Symbol	Levels		
		−1	0	1
Contact time (min)	A	60	120	180
Temperature (°C)	B	25	30	35
Adsorbent mass (m)	C	0.1	0.175	0.25
Sulfur concentration (ppm)	D	100	175	250

Results and discussion

Characterization of the adsorbent

The results obtained in the immediate analysis indicate that the schist shale has high ash content and low moisture and carbon content. The moisture content was 2.29%. The fixed carbon content, which is the fuel residue left after release of the volatile material from the oil shale ash sample, showed 1.33%. It may be primarily composed of carbon, although it may contain other elements not released during volatilization.

The ash content showed a high percentage of inorganic material, about 75%, which encompasses all minerals and is basically composed of oxides such as alumina, calcium oxide, silicon dioxide, etc. The volatile material content, approximately 21.38, portion separates into gaseous form, is composed of hydrocarbons optionally present in the solid structure and other gases, such as carbon monoxide.

The chemical analysis of Zn/X samples by X-ray fluorescence showed that it comprises a greater amount of Fe, Si, and Al, 33.9, 27.3, and 8.6% respectively, but also in the presence of various inorganic compounds in minor amounts, such as calcium, potassium, sulfur, titanium, magnesium, and strontium, among others, 4.6, 4.1, 2.3, and 4.9% respectively. The loss to fire was 14.3% of the composition of the Zn/X sample. According to the data, there is presence of Zn in the shale samples impregnated with the metal salt which was identified.

Figure 1 depicts the TG/DTG curves of Zn/X. They can be divided into three mass loss events, from 25 to 240, 240 to 550, and 550 to 900 °C. The first region with temperature up to 240 °C and mass loss of approximately 3% is relative to the removal of water present on the outer and inner surfaces of the clay minerals. The organic residues still present and the pyrite were decomposed in the second region, where it presented the largest mass loss of approximately 21% at the temperature of 550 °C. The loss of mass in the region above 550 °C is attributed to the decomposition of carbonate minerals.

The loss of total mass of Zn/X to 900 °C was 22.79%, indicating that the metal-impregnated shale showed a large amount of ash. This confirms the immediate analysis that revealed the value of 75% of inorganic material. This conclusion

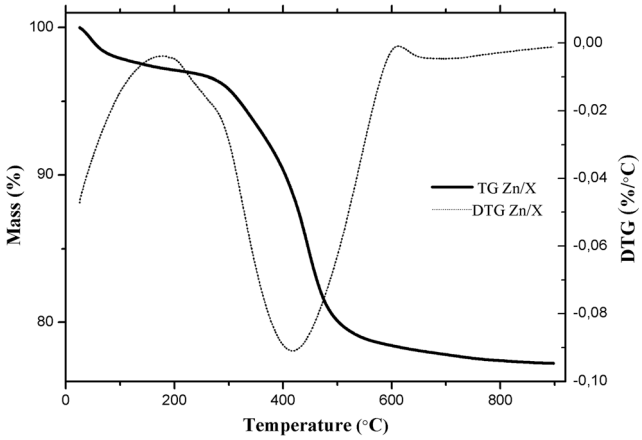

Fig. 1 Thermogravimetric curve of Zn/X samples

was due to the large amount of material for thiophene to act as an n-type donor by donating the solitary electron pair of the sulfur atom to the Zn/X (direct S-adsorbent or direct S-metal (σ) bond) or as a donor type of π using the electrons displaced from the aromatic ring to form a π complex with the adsorbent (Tang and Shi 2011).

Figure 2 shows the micrograph of the Zn-impregnated shale. The porous character of the material and particles with lamellar plate characteristic of clay minerals can be observed.

Adsorption kinetics

Kinetic adsorption studies provide valuable information about the mechanism of the adsorption process. The adsorption experiments were carried out at the concentrations of 250 ppm of S in contact with 0.1 g of adsorbent at the intervals of 5–300 min. The sulfur adsorption time variation was attributed in Fig. 3a in order to probe the sulfur adsorption kinetics in Zn/X.

The quantitative validation requires that the correlation coefficients be compared and can be verified by the linear graphs of each equation referring to the respective kinetic model. Considering the adsorption mechanism, in the present study, the kinetic models frequently used, namely pseudo first-order, pseudo second-order, and intraparticle diffusion models, were tested to investigate sulfur adsorption on Zn-impregnated shale as can be seen in Fig. 3b, c, d, respectively.

The adsorption in the model fuel increases with the time of contact and reaches saturation around 3 h in the three adsorbents; therefore, this was a fixed time limit for the adsorption of sulfur (Fig. 3a).

Correspondingly, the calculated values of the kinetic model are summarized in Table 2. The quantitative evaluation of the pseudo first-order and pseudo second-order models were performed by comparing the values of correlation coefficients (R^2). As shown in Fig. 3b, c and Table 2, both models generally provide a good fit quality; however, the pseudo second-order model has the value of $R^2 = 0.9942$ describing the experimental results better when compared to the pseudo first-order kinetic model with $R^2 = 0.9468$. Indicating that the sulfur-Zn/X system must be involved in an activated adsorption mechanism or chemisorption (Ho and McKay 1998).

Therefore, the adsorption of sulfur in Zn/X presented a higher correlation coefficient with the pseudo second-order kinetic model. And this model suggests that two reactions are occurring, in series or in parallel, being faster, causing the equilibrium to be reached quickly, and a slower one, which can continue for a long period of time (Behnamfard and Salarirad 2009). Aslam et al. (2017) and Danmaliki and Saleh (2017) reported that the pseudo second-order kinetics was the reaction rate that best described the adsorption of thiophene in the studied adsorbents. Nuntang et al. (2008) reported that the adsorption of thiophene on NaY or HUSY zeolites

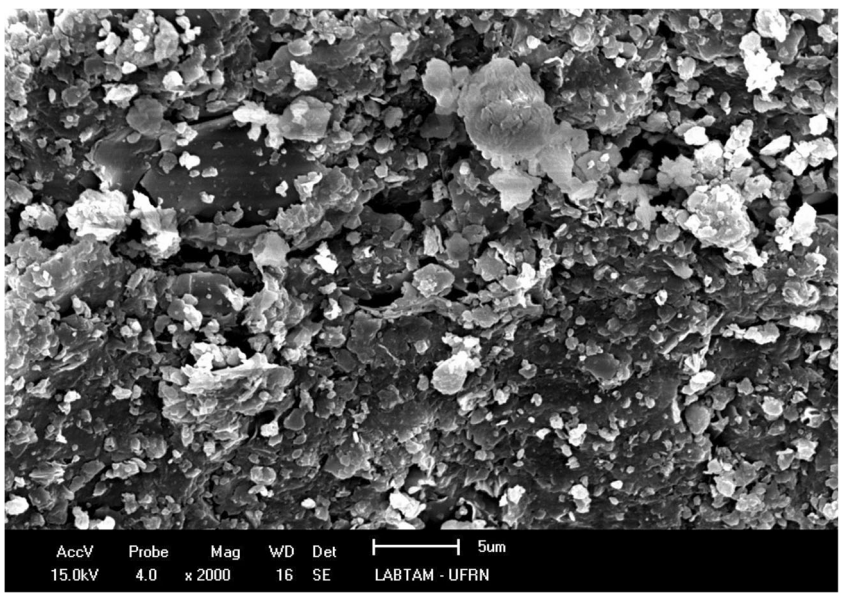

Fig. 2 Micrography × 2000 magnified Zn/X

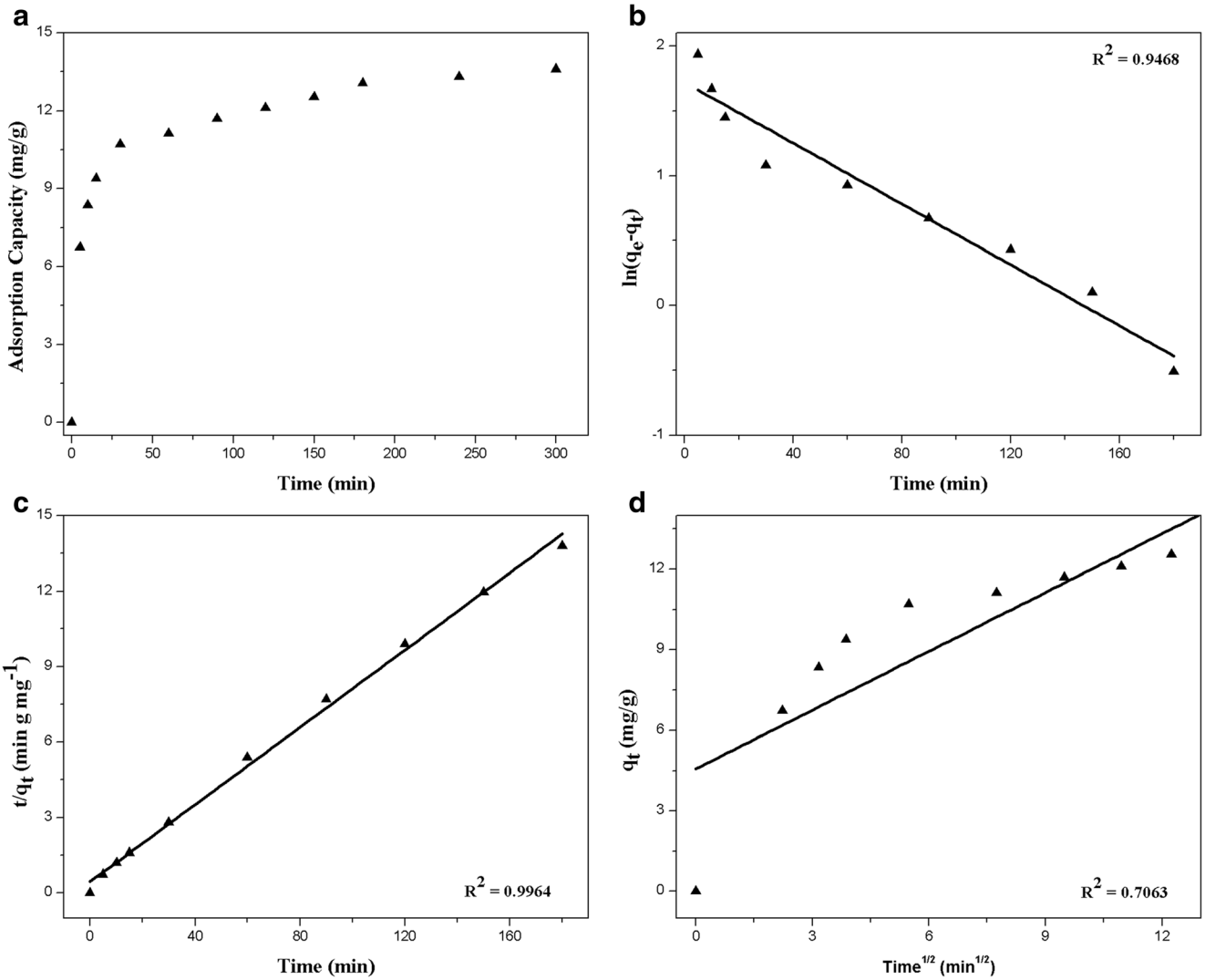

Fig. 3 Kinetic adsorption model. **a** Experimental points, **b** pseudo first order, (**c**) pseudo second order and (d) intraparticle diffusion

strongly depends on the electron densities in sulfur atom and thiophene aromatic ring due to the different interaction mechanisms between the sulfur-containing compositions and the adsorbent (direct S-M and π complexation).

As the pseudo second-order model is not able to identify the diffusion mechanism, the intraparticle diffusion model, based on the theory proposed by Weber and Morris (1963), was used. According to the authors, when intraparticle diffusion is the dominant mechanism in the adsorption process, the plot of adsorbed quantity (q_t) versus $t^{1/2}$ should result in a straight line (Behnamfard and Salarirad 2009). Figure 3d represents q_t versus $t^{1/2}$ for adsorption of sulfur in Zn/X. In this figure, the graph is not linear throughout the process, implying that more than one step is controlling the adsorption process and suggesting that the intraparticle diffusion mechanism is not dominant throughout the process.

Table 2 Kinetic and isotherms parameters for sulfur removal using Zn/X as adsorbent

Pseudo first order			Pseudo second order			Intraparticle diffusion		
$q_{e,calc}$ (mg/g)	k_1 (min^{-1})	R^2	$q_{e,calc}$ (mg/g)	k_2 (g/mg min)	R^2	$k_{i,3}$ (mg/g $min^{1/2}$)	C_3 (mg/g)	R^2
17.191	−0.0117	0.9468	0.4421	0.0767	0.9942	0.7302	4.5618	0.7063
Langmuir					Freundlich			
q_{max} (mg g^{-1})	K_L (dm^3 mg^{-1})	R^2	1/n	K_F (mg g^{-1}) (L $mg^{-1})^{1/n}$	R^2			
19.652	0.014	0.9689	0.565	0.783	0.9818			

The experimental data concerning the study of sulfur adsorption in Zn/X presented in Table 2 confirm that they did not fit the intraparticle diffusion model with low correlation coefficient ($R^2 = 0.7063$). The value of C (4.5618) other than 0 indicated that the lines q_t versus $t^{1/2}$ do not pass through the origin. Therefore, the intraparticle diffusion mechanism is not the speed-determining step and in the process of mass transfer other mechanisms must simultaneously act in the control of the adsorption process (Weber and Morris 1963).

Adsorption isotherms

An adsorption isotherm describes the relationship between the amount of adsorbate adsorbed by the adsorbent and the concentration of adsorbate remaining in the solution. There are several equations for analyzing experimental equilibrium adsorption data. In this work, the models of Langmuir and Freundlich were tested.

The Langmuir model assumes that the surface of the adsorbent has identical energetic sites and that each adsorbate molecule occupies a single site. This consequently provides for the formation of a monolayer of adsorbate coverage on the surface of the adsorbent. On the other hand, the Freundlich model describes a heterogeneous reversible adsorption, since it does not restrict to a monolayer of adsorbent cover (McKay 1996).

Figure 4 represents the sulfur adsorption isotherm at Zn/X, where the values obtained experimentally and the curves reached from the values estimated by the Langmuir and Freundlich models are presented.

Figure 4 shows the amount of sulfur adsorbed on the Zn/X surface and its concentration in the equilibrium model solution. This relationship showed that the adsorption capacity increases with the sulfur concentration in the model solution, progressively reaching saturation at high concentrations.

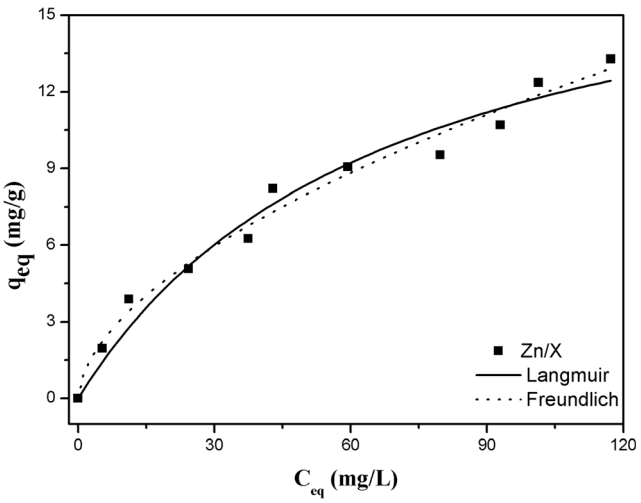

Fig. 4 Sulfur adsorption isotherms and non-linear Freundlich and Langmuir Zn/X adjustments

Analysis of the results based on the R^2 value for the two isotherms equations shows that the data is relatively close in both models. However, the Freundlich model was the one that best fits the studied adsorbent (Zn/X). This model presented a higher value of correlation coefficient (R^2), which means that the adjustment to the isotherm model was closer to that measured experimentally.

This behavior was the inverse presented by Subhan et al. (2014) who reported that adsorption isotherms showed a high regression coefficient and indication to the Langmuir model is somewhat more adequate to the Freundlich model to describe the adsorption equilibrium of the data using the Cu-KIT-6 adsorbent.

From the Langmuir isotherm adjustment, the maximum adsorption amount of Zn/X and the adsorption constant were calculated as 19.652 mg g^{-1} and 0.014 dm^3 mg^{-1}, with a correlation coefficient of 0.9689. This value indicates that this is a satisfactory adsorbent for sulfur removal in a hexane/toluene solution.

It can be seen that the Freundlich isotherm parameters of K_F and 1/n for sulfur adsorption of 0.773 and 0.565 (Table 2), respectively, determine a favorable adsorption process for the adsorbent studied, since 1/n presented a value less than 1.

Development of the regression model equation for sulfur removal

The optimization of experimental variables in the sulfur adsorption of the model fuel was performed using a complete factorial design 2^4 of two levels and three repetitions in the central point. The four variables considered as factors were the agitation time (A, min), temperature (B, °C), adsorbent mass (C, g), and sulfur concentration (D, ppm). The experimental matrix of the four factors on the response variable percent sulfur removal is presented in Table 3 for the Zn/X adsorbent. The randomness of the tests allows the balancing of the measurements and avoids possible confusion in the evaluation of the results.

This factorial project resulted in 19 tests with the possible combinations of A, B, C, and D. The coded mathematical model can be given as in Eq. (8):

$$\begin{aligned} Y_i = {} & a_0 + a_1X_{1i} + a_2X_{2i} + a_3X_{3i} + a_4X_{4i} + a_{12}X_{1i}X_{2i} \\ & + a_{13}X_{1i}X_{3i} + a_{14}X_{1i}X_{4i} + a_{23}X_{2i}X_{3i} + a_{24}X_{2i}X_{4i} \\ & + a_{34}X_{3i}X_{4i} + a_{123}X_{1i}X_{2i}X_{3i} + a_{124}X_{1i}X_{2i}X_{4i} \\ & + a_{134}X_{1i}X_{3i}X_{4i} + a_{234}X_{2i}X_{3i}X_{4i} \end{aligned} \quad (8)$$

The main and interaction coefficients were calculated by the following relation (Eqs. (9), (10), (11)) (SAHOO et al. 2001):

Table 3 The design matrix and the analysis of the complete factorial planning 2^4 with three central points

Standard execution	Factors				Experimental values
	A Time (min)	B Temperature (°C)	C Mass (g)	D Concentration *S* (ppm)	% remotion Zn/X
4					
1	− 1	− 1	− 1	− 1	57.54
16	1	1	1	1	44.67
7	− 1	1	1	− 1	52.11
5	− 1	− 1	1	− 1	62.32
10	1	− 1	− 1	1	57.02
2	1	− 1	− 1	− 1	64.02
8	1	1	1	− 1	68.41
13	− 1	− 1	1	1	41.10
19 (C)	0	0	0	0	53.10
11	− 1	1	− 1	1	38.84
12	1	1	− 1	1	44.24
17 (C)	0	0	0	0	51.74
14	1	− 1	1	1	54.56
18 (C)	0	0	0	0	59.52
3	− 1	1	− 1	− 1	61.47
15	− 1	1	1	1	54.45
9	− 1	− 1	− 1	1	53.15
6	1	− 1	1	− 1	55.22

$$a_0 = \sum \frac{Y_i}{N} \tag{9}$$

$$a_j = \sum \frac{X_{ji} Y_i}{N} \tag{10}$$

$$b_{nj} = \sum \frac{\left(X_{ni} X_{ji}\right) Y_i}{N} \tag{11}$$

Y_i is the response (% sulfur removal) and values of X_{ji} (j = 1, 2, 3; i = 1, 2, 3 ... 19) represent the corresponding parameters in their codified forms (Table 4); a_0 is the value of the average of the results obtained for the percent of sulfur removal; a_1, a_2, a_3, and a_4 are the linear coefficients (independent parameters); a_{12}, a_{13}, a_{23}, a_{24}, a_{34}, a_{123}, a_{124}, a_{134}, and a_{234} are the interaction coefficients and N is the number of total assays. The coefficients a_{12}, a_{13}, a_{23}, a_{24}, and a_{34} show the interaction effects of two variables at a time and a_{123}, a_{124}, a_{134}, and a_{234} show the interaction effects of three variables taken at a time.

In order to identify effective factors and interactions, a complete factorial planning 2^4 (Regti et al. 2017) is used. All experiments were performed in random order to evaluate the pure error method with three interactions and a significance level of 5% (α) to minimize the effect of possible uncontrolled variable (s). The regression coefficients of the independent variables having a response to percent sulfur removal using Zn/X are shown in Table 4.

Analyzing Table 4, three main factors were considered statistically significant: the adsorbent × adsorption contact time, the adsorbent mass, and the initial sulfur concentration. And three interactions, time × mass, temperature × mass and time × temperature × concentration, were considered statistically significant. Only the acquisition of this information justifies the use of statistical planning of experiments on the conventional univariate optimization procedure. This information would never have been obtained in a univariate optimization of the adsorption process.

The values of these coefficients were incorporated in Eq. (12), which assumes the following form:

$$\begin{aligned} Y_{\text{predicted}} = {} & 54.146 + 1.933A + 0.036B \\ & + 5.759C - 3.551D + 0.464AB - 1.450AC \\ & + 0.838AD + 3.435BC + 0.409BD \\ & + 0.491CD \\ & + 0.638ABC - 1.398ABD - 0.128ACD - 0.209BCD \end{aligned} \tag{12}$$

The effects of the individual variables and the effects of the interactions were estimated in Eq. (12), in which time, temperature, and adsorbent mass have a positive effect on adsorption of sulfur in the range of each selected variable for the present study. On the other hand, the greatest effect on sulfur removal was provided by the adsorbent mass. The interactions between time × mass, time × temperature × concentration,

Table 4 Coefficients of regression of the complete factorial planning 2^4

Terms	Regression coefficients	Square effects	*t* (2)	*p*	Lim coef −95%	Lim coef +95%
Average	*54.14684*	*0.240026*				
A	*1.93313*	*0.261562*	*7.3907*	*0.017820*	*0.80772*	*3.05853*
B	0.03687	0.261562	0.1410	0.900804	− 1.08853	1.16228
C	*5.75938*	*0.261562*	*22.0192*	*0.002056*	*4.63397*	*6.88478*
D	*− 3.55188*	*0.261562*	*− 13.5795*	*0.005379*	*− 4.67728*	*− 2.42647*
AB	0.46437	0.261562	1.7754	0.217822	− 0.66103	1.58978
AC	*− 1.45063*	*0.261562*	*− 5.5460*	*0.031007*	*− 2.57603*	*− 0.32522*
AD	0.83813	0.261562	3.2043	0.085140	− 0.28728	1.96353
BC	*3.43563*	*0.261562*	*13.1350*	*0.005746*	*2.31022*	*4.56103*
BD	0.40938	0.261562	1.5651	0.258029	− 0.71603	1.53478
CD	0.49188	0.261562	1.8805	0.200779	− 0.63353	1.61728
ABC	0.63813	0.261562	2.4397	0.134846	− 0.48728	1.76353
ABD	*− 1.39813*	*0.261562*	*− 5.3453*	*0.033263*	*− 2.52353*	*− 0.27272*
ACD	− 0.12813	0.261562	− 0.4898	0.672704	− 1.25353	0.99728
BCD	− 0.20938	0.261562	− 0.8005	0.507410	− 1.33478	0.91603

Statistically significant factors were italicized

time × mass × concentration, and temperature × mass × concentration have a negative effect on the removal of sulfur.

The corresponding *P* value less than 0.05 indicates that the model is statistically significant (Farooq et al. 2017). The effects and estimated coefficients for this model are listed in Table 4. The results showed that the factors of contact time (A), adsorbent mass (C), and initial sulfur concentration (D) have a very small *P* value (ACD), temperature × mass (BC), and three time × temperature × concentration (ABD) interactions. An appropriate model can be expressed as can be seen in Eq. (13):

$$Y_{\text{predicted}} = 54.146 + 1.933A + 5.759C - 3.551D - 1.450AC + 3.435BC - 1.398ABD \quad (13)$$

Analysis of variance

After estimating the main effects, interaction factors affecting sulfur removal, and proof of significance, the adequacy of the regression was determined by performing the variance (ANOVA) analysis. In this analysis, a significance level of 5% (α) was used to statistically verify the variation of the experimental results produced by some factor (s). The tests were performed with the F statistic. The synthesis of results is presented in Table 5.

The most used method to evaluate the fit quality of a model is the analysis of variance obtained from the quadratic mean values. To consider the significant model, the value of F_{calc} ($MS_{\text{regression}}/MS_{\text{residuals}}$) must be greater than the value of F_{tab}. The larger this value, the more evidence you have that you can consider the regression to be useful for forecasting purposes, while the value of the F_{calc} ($MS_{\text{lack of fit}}/MS_{\text{pure error}}$) must be less than the value of F_{tab}.

From the data shown in Table 5, we see that the ratio $MS_{\text{regression}}/MS_{\text{residual}}$ (131.028) is much higher than the table value of $F_{0.95;14;4}$ (5.873), at 95% confidence, and ratio $MS_{\text{lack of fit}}/MS_{\text{pure error}}$ (0.071) is much smaller than the value of $F_{0.95;2;2}$ (19). With this, we can affirm the good quality of the model obtained for the prediction of the yield of the reaction.

The analysis of the ANOVA (Table 5) shows that the proposed model has statistical significance, at the 95% confidence level, since the calculated value of F (regression/residues) is approximately 20 times greater than $F_{0.95;14;4}$ tabulated (5.873). It is clear that the F_{cal} values for the regression are larger than the F_{tab}, which implies that most of the variation in the response can be explained by regression modeling (ROOSTA et al. 2014).

The R^2 obtained suggests good adjustments to the model for the experimental results, since these indicate that 99.97% of the variability that the response could be explained. R^2 (adjusted R^2) (Eq. (14)) is also a good measure of an adjustment, but it is more appropriate to compare the model with different numbers of independent variables. It corrects the R^2 value for the sample size and the number of terms in the model using the degrees of freedom in its computation. So, if there are many terms in a model and not too large of a sample size, adjusted R^2 may be less visible than R^2 (Meski et al. 2011). Here, the adjusted R^2 value (99.02%) is closer to the corresponding R^2 value. All of these tests verify the fact that the model does not violate the premise regression.

$$\text{Adj}R^2 = R^2 - \left(1 - R^2\right)\frac{(l-1)}{(N-1)} \quad (14)$$

Table 5 ANOVA results for complete factorial planning 2^4

Source of variation	Sum of squares (SS)	Degrees of freedom	Mean square (MS)	F_{cal}	F_{tab}
Regression	1074.915	14	76.780	131.028	5.873
Residuals	2.344	4	0.586		
Lack of fit	0.155	2	0.077	0.071	19
Pure error	2.189	2	1.094		
Total	1077.259	18			
R^2	0.9997				
Adjusted R^2	0.9902				

Table 6 presents the experimental values of the percentage of sulfur removal and the values predicted by the coded model that was validated by ANOVA as well as the relative error of each test, quantifying the percentage of the experimental value less predicted by the model in relation to the experimental one.

Observing Table 6, it is noted that the predicted percentage of sulfur removal values are close to the percentage of sulfur removal obtained experimentally, where the deviations relative to most of the experiments were less than about 0.1%, and only two experiments showed deviations of approximately 1% indicating that the statistical analysis performed at 95% and ANOVA is valid and has a good fit of the model.

Residuals analysis

The residual also has to be examined for normal distribution. The Anderson-Darling test is a powerful statistical medium that generates normal probability plot and performs a hypothesis test to examine whether observations follow a normal distribution.

Figure 5 shows a distribution of residual values, defined as values between predicted values (model) and observed values (experimental). As can be seen, the residues follow a normal distribution, with two negative residues (below 50%) and three positive residues (above 50%). For this, the maximum deviation and minimum values of zero is only ± 1.073, which indicates the model presents a minimum adjusted value of the observed value. Figure 5 indicates that a straight line can be adjusted indicating the model follows a normal distribution (Myers et al. 2009).

The plot of standard residuals versus predicted values indicates the possible existence of atypical values (Fig. 6). If a point is far from most points, it can be an excessive value. It is important to identify atypical values because they can influence the model, potentially providing misleading or incorrect results.

Table 6 Percentage values of experimental sulfur removal predicted by the model and relative deviations for the 19 full factorial design trials 2^4

Run	Experimental values	Predicted values	Relative deviation (%)
1	55.31	55.256	0.054
2	57.54	57.642	−0.102
3	44.67	44.772	−0.102
4	52.11	52.056	0.054
5	62.32	62.422	−0.102
6	57.02	56.966	0.054
7	64.02	63.966	0.054
8	68.41	68.512	−0.102
9	41.10	41.202	−0.102
10	53.10	53.046	0.054
11	38.84	38.786	0.054
12	44.24	44.342	−0.102
13	51.74	51.686	0.054
14	54.56	54.662	−0.102
15	59.52	59.622	−0.102
16	61.47	61.416	0.054
17 (C)	54.45	54.147	0.303
18 (C)	53.15	54.147	−0.997
19 (C)	55.22	54.147	1.073

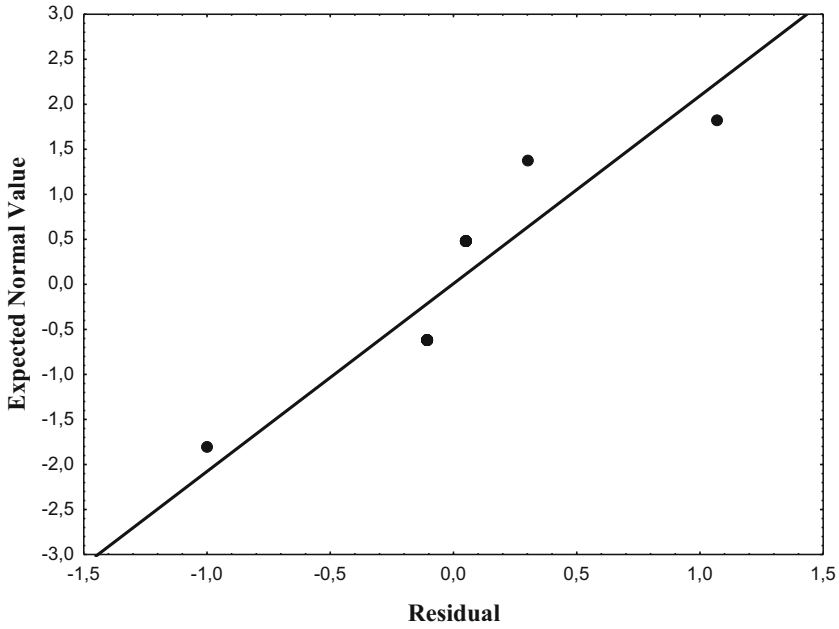

Fig. 5 The normality plot of residuals

As can be seen, the graph of the residues (Fig. 6) revealed that they do not have an obvious pattern and unusual structure. Almost all standardized residues were randomly scattered across the graph. This implies that the proposed model is adequate and that there is no reason to suspect any breach of independence or constant variance hypothesis, since all points were found in the range of +1.5 to −1.5.

Pareto diagram and main effects

Fig.7 represents the Pareto diagram of this experimental design that shows the influence of important factors in the removal effectively. The significance of the factors and their interactions were obtained using a Student *t* test with a confidence interval of 95%. Values that exceed a baseline are considered as significant factors.

It can be seen from Fig. 7 that the main factors C, D, and A, and the interaction effect BC, AC, and ABD that extend beyond the reference line, are significant at the 0.05 level. The adsorbent mass (C) represented the most significant effect on sulfur adsorption efficiency. The initial sulfur concentration (D), time (A), and temperature × mass (BC) interaction have great effects on adsorption efficiency. Although, the interaction effects between AC and ABD have a significant effect and are statistically significant at the 95% confidence level.

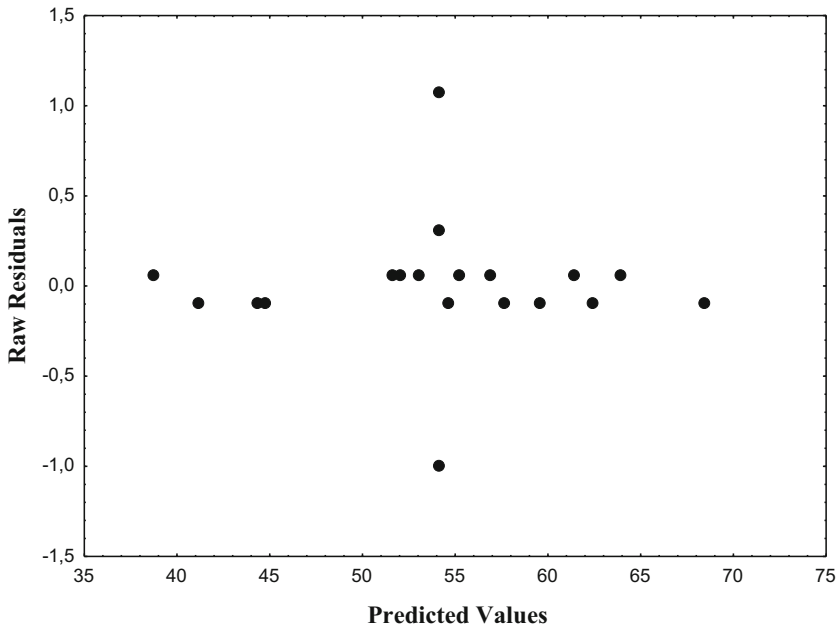

Fig. 6 Expected values of percentage sulfur removal versus residues

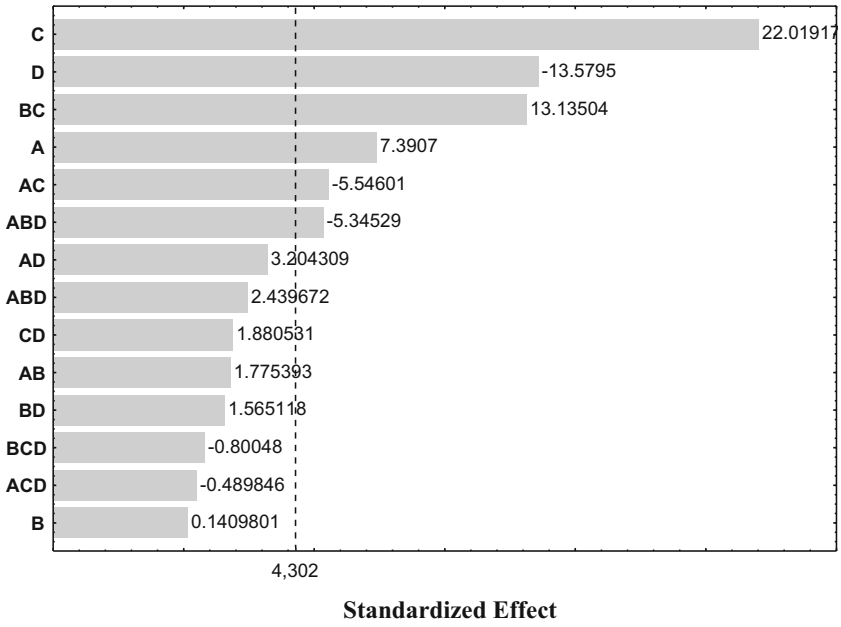

Fig. 7 Pareto diagram of complete factorial planning 2^4

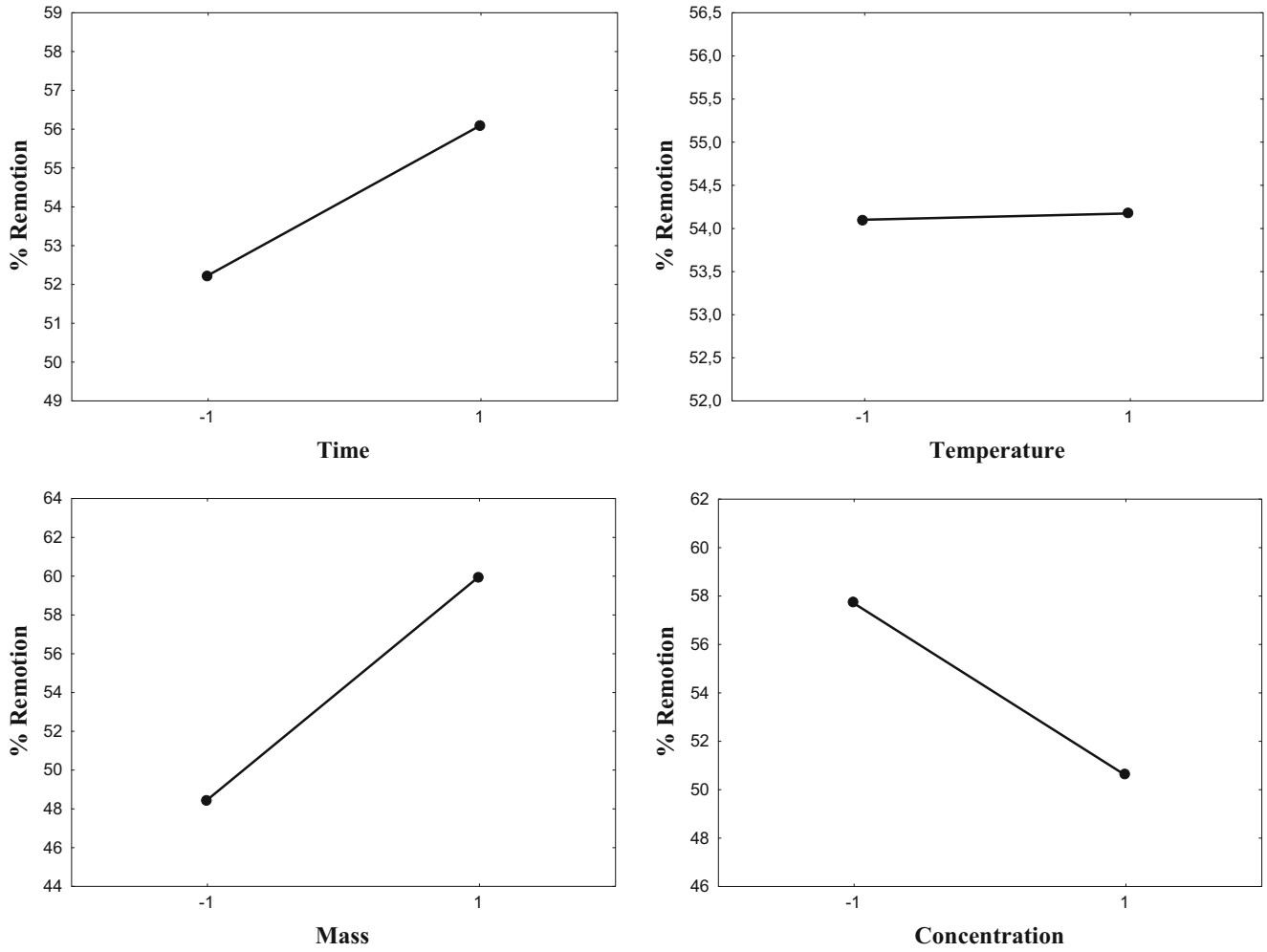

Fig. 8 Main effect graph for percentage of sulfur removal

According to the Pareto diagram, it can be inferred that the adsorbent mass was the most important variable for the general optimization of the overall sulfur adsorption process, since it influenced more significantly reaching an estimated effect of approximately 22.0191. The sequence of major importance of the main factors and their interactions can be expressed as C > D > BC > A > AC > ABD > AD > ABC > CD > AB > BD > BCD > ACD > B, following a decreasing influence on the adsorbed amount of sulfur. The last eight in the sequence are considered insignificant.

All adsorption experiments were performed on the specified combinations of the working variables using statistically designed patterns of experience to evaluate the interactions of these variable factors. Figure 8 shows the main effects of control factors after adsorption of sulfur.

It is evident from Fig. 8 that the variables considered for the design of a model play a relevant role in the investigation of sulfur adsorption since each variable has a considerable contribution in the removal of sulfur. Specifically, the main effects show mean variations between the high and low values of each factor. The magnitude of the slope represents the intensity of the effects that each factor exerts. When the slope is positive, an increase in removal efficiency occurs for the high level of this factor and vice versa.

It can be seen in Fig. 8 that the effect of the initial sulfur concentration was characterized by a high degree of starting and also had a negative effect on the response, whereas the time and mass of the adsorbent had a positive effect on the response with a greater match. Then the percent of sulfur removal appears to be significantly affected by the increase in the time period from 60 to 180 min and the adsorbent mass from 0.1 to 0.25 g. The addition of contact time and adsorbent mass implies an increase in adsorption efficiency. Also, the adsorption is favored with the concentration of lower level (100 ppm).

Conclusion

Experimental results indicated that Zn-impregnated shale can be a low-cost material alternative for sulfur removal in model fuel. The Freundlich equation describes well the equilibrium isotherm. The adsorption kinetics can be described by a pseudo second-order model. The study identified the significant variables, the interaction between them, and in particular, the optimal conditions of the variables for the maximum sulfur removal through ANOVA, *t* test, and *F* test. The optimum set of conditions for the maximum adsorption of sulfur in Zn/X was as follows: contact time = 180 min, temperature = 35 °C, adsorbent mass = 0.25 g, and initial sulfur concentration = 100 ppm. The R^2 value 99.97% indicates a good fit of the model. The experimental values were in good agreement with the predicted values of the model.

References

Ahmad Y, Danish M, Rafatullah M, Arniza G, Sulaiman O, Hashim R, Nasir M, Ibrahim M (2011) The use of date palm as a potential adsorbent for wastewater treatment: a review. Environ Sci Pollut Res 19:1464–1484. https://doi.org/10.1007/s11356-011-0709-8

ANP (2016) Agência Nacional do Petróleo, Gás Natural e Biocombustíveis. Qualidade. http://www.anp.gov.br/anexos/154D4048F327E20783257C510055D721/graficos_teor_de_enxofre.docx. Accessed 21 June 2017

Aslam S, Sbhan F, Yan Z, Etim UJ, Zeng J (2017) Dispersion of nickel nanoparticles in the cages of metal-organic framework: an efficient sorbent for adsorptive removal of thiophene. Chem Eng J 315:469–480. https://doi.org/10.1016/j.cej.2017.01.047

ASTM D3172 (2013) Standard practice for proximate analysis of coal and coke, ASTM International, West Conshohocken, PA, www.astm.org. Accessed 01 July 2017

ASTM D3173 (2017) Standard test method for moisture in the analysis sample of coal and coke, ASTM International, West Conshohocken, PA, www.astm.org. Accessed 01 July 2017

ASTM D3174 (2012) Standard test method for ash in the analysis sample of coal and coke from coal, ASTM International, West Conshohocken, PA, www.astm.org. Accessed 01 July 2017

ASTM D3175 (2017) Standard test method for volatile matter in the analysis sample of coal and coke, ASTM International, West Conshohocken, PA, www.astm.org. Accessed 01 July 2017

Baeza P, Aguila G, Vargas G, Ojeda J, Araya P (2012) Adsorption of thiophene and dibenzothiophene on highly dispersed Cu/ZrO2 adsorbents. Appl Catal B Environ 111-112:133–140. https://doi.org/10.1016/j.apcatb.2011.09.026

Behnamfard A, Salarirad MM (2009) Equilibrium and kinetic studies on free cyanide adsorption from aqueous solution by activated carbon. J Hazard Mater 170:127–133. https://doi.org/10.1016/j.jhazmat.2009.04.124

Bhandari VM, Ko CH, Geun PJ, Han SS, Cho SH, Kim N (2006) Desulfurization of diesel using ion-exchanged zeolites. Chem Eng Sci 61:2599–2608. https://doi.org/10.1016/j.ces.2005.11.015

Bhatia S, Sharma DK (2012) Thermophilic desulfurization of dibenzothiophene and different petroleum oils by Klebsiella sp. 13T. Environ Sci Pollut Res 19:491–3497

Blanco-Brieva G, Campos-Martim JM, Al-Zahrani SM, Fierro JLG (2011) Effectiveness of metal–organic frameworks for removal of refractory organo-sulfur compound present in liquid fuels. Fuel 90:190–197. https://doi.org/10.1016/j.fuel.2010.08.008

Brunet S, Mey D, Péron G, Bouchy C, Diehl F (2005) On the hydrodesulfurization of FCC gasoline: a review. Appl Catal A Gen 278:143–172. https://doi.org/10.1016/j.apcata.2004.10.012

Cavalcanti RM, Wanilson AGPJ, Braga VS, Barros ICL (2015) Adsorption of sulfur compound utilizing rice husk ash modified with niobium. Appl Surf Sci 355:171–182. https://doi.org/10.1016/j.apsusc.2015.07.129

Chen TC, Agripa ML, Lu MC, Dalila MLP (2016) Adsorption of sulfur compounds from diesel with ion-impregnated activated carbons. Energy Fuel 30:3870–3878. https://doi.org/10.1021/acs.energyfuels.6b00230

Danmaliki GI, Saleh TA (2017) Effects of bimetallic Ce/Fe nanoparticles on the desulfurization of thiophenes using activated carbon. Chem Eng J 307:914–927. https://doi.org/10.1016/j.cej.2016.08.143

Dharaskar SA, Wasewar KL, Varma MN, Shende DZ, Tadi KK, Yoo CK (2014) Synthesis, characterization, and application of novel trihexyl tetradecyl phosphonium bis (2,4,4-trimethylpentyl) phosphinate for extractive desulfurization of liquid fuel. Fuel Process Technol 123:1–10. https://doi.org/10.1016/j.fuproc.2014.02.001

Dharaskar SA, Wasewar KL, Varma MN, Shende DZ (2016) Synthesis, characterization, and application of 1-butyl-3-methylimidazolium

thiocyanate for extractive desulfurization of liquid fuel. Environ Sci Pollut Res 23:9284–9294. https://doi.org/10.1007/s11356-015-4945-1

Duarte FA, Mello PA, Bizzi CA, Nunes MAG, Moreira EM, Alencar MA, Motta HN, Dressler VL, Flores EMM (2011) Sulfur removal from hydrotreated petroleum fractions using ultrasound-assisted oxidative desulfurization process. Fuel 90:2158–2164. https://doi.org/10.1016/j.fuel.2011.01.030

Farooq S, Saeed A, Sharif M, Hussain J, Mabood F, Iftekhar M (2017) Process optimization studies of crystal violet dye adsorption onto novel, mixed metal Ni 0.5 Co 0.5 Fe 2 O 4 ferrospinel nanoparticles using factorial design. J Water Process Eng 16:132–141. https://doi.org/10.1016/j.jwpe.2017.01.001

Gao H, Guo C, Xing J, Zhao J, Liu H (2010) Extraction and oxidative desulfurization of diesel fuel catalyzed by a Brønsted acidic ionic liquid at room temperature. Green Chem 12:1220–1224. https://doi.org/10.1039/c002108c

Gui J, Liu D, Sun Z, Liu D, Min D, Song B, Peng X (2010) Deep oxidative desulfurization with task-specific ionic liquids: an experimental and computational study. J Mol Catal A Chem 331:64–70. https://doi.org/10.1016/j.molcata.2010.08.003

He C, Men G, Xu B, Cui J, Zhao J (2016) Phenolic resin-derived activated carbon-supported divalent metal as efficient adsorbents (M–C, M=Zn, Ni, or Cu) for dibenzothiophene removal. Environ Sci Pollut Res 24:782–794. https://doi.org/10.1007/s11356-016-7795-6

Ho YS, Mckay G (1998) Sorption of dye from aqueous solution by peat. Chem Eng J 70:115–124. https://doi.org/10.1016/s0923-0467(98)00076-1

Iberahim N, Sethupathi S. Bashir, MJK (2017) Optimization of palm oil mill sludge biochar preparation for sulfur dioxide removal. Environ Sci Pollut Res. Springer Nature. 26: 1–13 doi: https://doi.org/10.1007/s11356-017-9180-5

Ibrahim RK, Hayyan M, AlSaadi MA, Hayyan A, Ibrahim S (2016) Environmental application of nanotechnology: air, soil, and water. Environ Sci Pollut Res 23:13754–13788. https://doi.org/10.1007/s11356-016-6457-z

James GS (2000) The desulfurization of heavy oils and residua, 2nd edn. Marcel Dekker Inc., New York

Komarneni M, Kadossov E, Justin J, Lu M, Burghaus U (2010) Adsorption of thiophene on silica-supported Mo clusters. Surface Science 604 (13-14):1221–1229

Kwon JM, Moon JH, Bae YS, Lee DG, Sohn HC, Lee CH (2008) Adsorptive desulfurization and denitrogenation of refinery fuels using mesoporous silica adsorbents. Wiley-Blackwell. ChemSusChem 4:307–309. https://doi.org/10.1002/cssc.200700011

Li Z, Barnes JC, Bosoy A, Stoddart JF, Zink JI (2012) Mesoporous silica nanoparticles in biomedical applications. Chem Soc Rev 41:2590–2605. https://doi.org/10.1039/c1cs15246g

Li CJ, Li YJ, Wang JN, Zhao L, Cheng J (2013) Ag^{+}-loaded polystyrene nanofibrous membranes preparation and their adsorption properties for thiophene. Chem Eng J 222:419–425. https://doi.org/10.1016/j.cej.2012.09.107

Lü H, Deng C, Ren W, Yang X (2014) Oxidative desulfurization of model diesel using $[(C_4H_9)4N]_6Mo_7O_{24}$ as a catalyst in ionic liquids. Fuel Process Technol 119:87–91. https://doi.org/10.1016/j.fuproc.2013.10.023

Ma X, Velu S, Kim JH, Song C (2005) Deep desulfurization of gasoline by selective adsorption over solid adsorbents and impact of analytical methods on ppm-level sulfur quantification for fuel cell applications. Appl Catal B Environ 56:137–147. https://doi.org/10.1016/j.apcatb.2004.08.013

Ma X, Zhou A, Song C (2007) A novel method for oxidative desulfurization of liquid hydrocarbon fuels based on catalytic oxidation using molecular oxygen coupled with selective adsorption. Catal Today 123:276–284. https://doi.org/10.1016/j.cattod.2007.02.036

McKay G (1996) Use of adsorbents for the removal of pollutants from wastewaters. CRC Press, Inc., Boca Raton

Meski S, Ziani S, Khireddine H, Boudboub S, Zaidi S (2011) Factorial design analysis for sorption of zinc on hydroxyapatite. J Hazard Mater 186:1007–1017. https://doi.org/10.1016/j.jhazmat.2010.11.087

Myers RH, Montgomery DC, Anderson-Cook CM (2009) Response surface methodology—process and product optimization using designed experiments, 3rd edn. John Wiley & Sons, Inc., Hoboken

Nejad NF, Beigi AAM (2015) Efficient desulfurization of gasoline fuel using ionic liquid extraction as a complementary process to adsorptive desulfurization. Pet Sci 12:330–339. https://doi.org/10.1007/s12182-015-0020-2

Nuntang S, Prasassarakich P, Ngamcharussrivichai C (2008) Comparative study on adsorptive removal of thiophenic sulfurs over Y and USY zeolites. Ind Eng Chem Res 47:7405–7413. https://doi.org/10.1021/ie701785s

Oliveira MLM, Miranda AAL, Barbosa CMBM, Cavalcante CL Jr, Azevedo DCS, Rodriguez-Castellon E (2009) Adsorption of thiophene and toluene on NaY zeolites exchanged with Ag(I), Ni(II) and Zn(II). Fuel 88:1885–1892. https://doi.org/10.1016/j.fuel.2009.04.011

Oyama ST, Gott T, Zhao H, Lee YK (2009) Transition metal phosphide hydroprocessing catalysts: a review. Catal Today 143:94–107. https://doi.org/10.1016/j.cattod.2008.09.019

Peralta D, Chaplais G, Simon-Masseron A, Barthelet K, Pirgngruber GD (2012) Metal–organic framework materials for desulfurization by adsorption. Energy Fuel 26:4953–4960. https://doi.org/10.1021/ja211864w

Pimentel PM, Melo MAF, Melo DMA, Assunção ALC, Henrique DM, Silva Jr CN, González G (2008) Kinetics and thermodynamics of Cu(II) adsorption on oil shale wastes. Fuel Process Technol 89:62–67. https://doi.org/10.1016/j.fuproc.2007.07.003

Pimentel PM, Oliveira RMPB, Melo DMA, Anjos MJ, Melo MAF, González G (2010) Characterization of retorted shale for use in heavy metal removal. Appl Clay Sci 48:375–378. https://doi.org/10.1016/j.clay.2010.01.009

Regti A, Laamari MR, Stiriba SE, El Haddad M (2017) Use of response factorial design for process optimization of basic dye adsorption onto activated carbon derived from Persea species. Microchem J 130:129–136. https://doi.org/10.1016/j.microc.2016.08.012

Roosta M, Ghaedi M, Shori N, Daneshfar A, Sahraei R, Asghari A (2014) Optimization of the combined ultrasonic assisted/adsorption method for the removal of malachite green by gold nanoparticles loaded on activated carbon: experimental design. Spectrochim Acta A Mol Biomol Spectrosc 118:55–65. https://doi.org/10.1016/j.saa.2013.08.082

Sahoo RN, Naik PK, Das SC (2001) Leaching of manganese from low-grade manganese ore using oxalic acid as reductant in sulphuric acid solution. Hydrometallurgy 62:157–163. https://doi.org/10.1016/s0304-386x(01)00196-7

Shi Y, Zhang W, Zhang H, Tian F, Jia C, Chen Y (2013) Effect of cyclohexene on thiophene adsorption over NaY and LaNaY zeolites. Fuel Process Technol 110:24–32. https://doi.org/10.1016/j.fuproc.2013.01.008

Shimoyama I, Baba Y (2016) Thiophene adsorption on phosphorus- and nitrogen-doped graphites: control of desulfurization properties of carbon materials by heteroatom doping. Carbon 98:115–125. https://doi.org/10.1016/j.carbon.2015.10.094

Song C (2003) An overview of new approaches to deep desulfurization for ultra-clean gasoline, diesel fuel and jet fuel. Catal Today 86:211–263. https://doi.org/10.1016/s0920-5861(03)00412-7

Srivastav A, Srivastava VC (2009) Adsorptive desulfurization by activated alumina. J Hazard Mater 170:1133–1140. https://doi.org/10.1016/j.jhazmat.2009.05.088

Stanislaus A, Marafi A, Rana MS (2010) Recent advances in the science and technology of ultra low sulfur diesel (ULSD) production. Catal Today 153:1–68. https://doi.org/10.1016/j.cattod.2010.05.011

Subhan F, Liu BS, Zhang QL, Wang WS (2012) Production of ultra-low-sulfur gasoline: an equilibrium and kinetic analysis on adsorption of sulfur compounds over Ni/MMS sorbents. J Hazard Mater 239-240: 370–380. https://doi.org/10.1016/j.jhazmat.2012.09.012

Subhan F, Aslam S, Yan Z, Ikram M, Rehman S (2014) Enhanced desulfurization characteristics of Cu-KIT-6 for thiophene. Microporous Mesoporous Mater 199:108–116. https://doi.org/10.1016/j.micromeso.2014.08.018

Tang X-L, Shi L (2011) Study of the adsorption reactions of thiophene on Cu(I)/HY-Al2O3by Fourier transform infrared and temperature-programmed desorption: adsorption, desorption, and sorbent regeneration mechanisms. Langmuir 27:11999–12007. https://doi.org/10.1021/la2025654

Teymouri M, Samadi-Maybodi A, Vahid A, Miranbeigi A (2013) Adsorptive desulfurization of low sulfur diesel fuel using palladium containing mesoporous silica synthesized via a novel in-situ approach. Fuel Process Technol 116:257–264. https://doi.org/10.1016/j.fuproc.2013.07.009

Tian F, Shen Q, Fu Z, Wu Y, Jia C (2014) Enhanced adsorption desulfurization performance over hierarchically structured zeolite Y. Fuel Process Technol 128:176–182. https://doi.org/10.1016/j.fuproc.2014.07.018

Tian F, Fu Z, Zhang H, Zhang J, Chen Y, Jia C (2015) Thiophene adsorption onto metal–organic framework HKUST-1 in the presence of toluene and cyclohexene. Fuel 158:200–206. https://doi.org/10.1016/j.fuel.2015.05.030

Topsøe H (2003) Developments in operando studies and in situ characterization of heterogeneous catalysts. J Catal 216:155–164. https://doi.org/10.1016/s0021-9517(02)00133-1

USEPA (2000) Regulatory announcement: heavy-duty engine and vehicle standards and highway fuel sulfur control requirements. www.archive.epa.gov/midwestcleandiesel/web/pdf/exec-sum.pdf. Accessed 03 July 2017

Velu S, Song C, Engelhard MH, Chin YH (2005) Adsorptive removal of organic sulfur compounds from jet fuel over K-exchanged NiY zeolites prepared by impregnation and ion exchange. Ind Eng Chem Res 44:5740–5749. https://doi.org/10.1021/ie0488492

Wang Y, Yang RT (2007) Desulfurization of liquid fuels by adsorption on carbon-based sorbents and ultrasound-assisted sorbent regeneration. Langmuir 23:3825–3831. https://doi.org/10.1021/la063364z

Wang H, Song L, Jian H, Xu J, Jin L, Zhang X, Sun Z (2009a) Effects of olefin on adsorptive desulfurization of gasoline over Ce(IV)Y zeolites. Fuel Process Technol 90:835–838. https://doi.org/10.1021/ie404362f

Wang Q, Liang X-y, Zhang R, Liu C-j, Liu X-j, Qiao W-m, Zhan L, Ling L-c (2009b) Preparation of polystyrene-based activated carbon spheres and their adsorption of dibenzothiophene. New Carbon Mater 24:55–60. https://doi.org/10.1016/s1872-5805(08)60036-0

Wang L, Zhao X, Zhang J, Xiong Z (2017) Selective adsorption of Pb (II) over the zinc-based MOFs in aqueous solution-kinetics, isotherms, and the ion exchange mechanism. Environ Sci Pollut Res 24:14198–14206. https://doi.org/10.1007/s11356-017-9002-9

Weber WJ, Morris JC (1963) Kinetics of adsorption on carbon from solution. J Sanit Eng Div 89:31–60

Wei SHH, Cheng Y, Yang C, Zeng G, Qiu L (2016) Performances, kinetics and mechanisms of catalytic oxidative desulfurization from oils. RSC Adv 6:103253–103269. https://doi.org/10.1039/c6ra22358c

Wei SHH, Cheng Y, Yang C, Zeng G, Kang L, Qian H, Zhu C (2017) Preparation, characterization, and catalytic performances of cobalt catalysts supported on KIT-6 silicas in oxidative desulfurization of dibenzothiophene. Fuel 200:11–21. https://doi.org/10.1016/j.fuel.2017.03.052

Wu L, Sitamraju S, Xiao J, Liu B, Li Z, Janik MJ, Song C (2014) Effect of liquid-phase O3 oxidation of activated carbon on the adsorption of thiophene. Chem Eng J 242:211–219. https://doi.org/10.1016/j.cej.2013.12.077

Xiao J, Wang X, Fujii M, Yang Q, Song C (2013) A novel approach for ultra-deep adsorptive desulfurization of diesel fuel over TiO2-CeO2/MCM-48 under ambient conditions. AICHE J 59:1441–1445. https://doi.org/10.1002/aic.14085

Yu T, Cheng P, Huang E, Wang P, Tian H (2015a) First-principle investigation of thiophene adsorption on TM (Ni/Co/Mn)-doped (ZnO)15 nanotube. Comput Theor Chem 1057:15–23. https://doi.org/10.1016/j.comptc.2015.01.008

Yu M, Zhang N, Fan L, Zhang C, Ele X, Zheng M, Li Z (2015b) Removal of organic sulfur compounds from diesel by adsorption on carbon materials. Rev Chem Eng 31:27–43. https://doi.org/10.1515/revce-2014-0017

Zhang S, Zhang Y, Huang E, Wang P, Tian H (2012) Mechanistic investigations on the adsorption of thiophene over Zn3NiO4 bimetallic oxide cluster. Appl Surf Sci 258:10148–10153. https://doi.org/10.1016/j.apsusc.2012.06.096

Zhang J, Tian Y, Yin L, Zuo W, Gong Z, Zhang J (2017) Investigation on the removal of H2S from microwave pyrolysis of sewage sludge by an integrated two-stage system. Environ Sci Pollut Res. Springer Nature 24:19920–19926. https://doi.org/10.1007/s11356-017-9637-6